

Fig. 5 Effect of tripping the boundary layer on reduced pressure distribution. Data taken from Dziomba.⁴

The trends shown in Fig. 4 are qualitatively similar to the effect of either tripping the boundary layer on the front face before it separates,⁴ or increasing the freestream turbulence level.^{1,3} Tripping of the boundary layer was reported⁴ to reduce the reattachment length by up to 40%, and the base pressure coefficient by 15%. The shortening of the bubble was attributed to an effective change in the separation angle due to the formation of a small recirculation bubble between the trip wires and the sharp leading edge of the plate.

To elucidate this point, the pressure distributions reported in Ref. 4 (measured at UBC using the same base model) were replotted in terms of reduced coordinates for the basic undisturbed flow and two tripped flows using different diameter wires. The results in Fig. 5 show that the collapse, though reasonable, is not as good as that obtained in Fig. 3 with the various leading-edge angles. In particular C_{p_m} increases from about 0.4 to 0.43 when the boundary layer is tripped, and the pressure recovery process starts earlier resulting in a shift of the data towards the left. This, together with the proportionally higher decrease in C_{p_b} noticed earlier, indicates that the effect of the trip wire may be partly due to an effective change in the separation angle, but it is not confined to this mechanism. Additional factors to be considered are possible changes in the state of the separating boundary layer and in the initial growth rate of the separated shear layer.

References

- ¹Hillier, R., and Cherry, N. J., "The Effect of Stream Turbulence on Separation Bubbles," *Journal of Wind Engineering and Industrial Aerodynamics*, Vol. 8, July 1981, pp. 49-58.
- ²Gartshore, I. S., and Savill, M., "Some Effects of Freestream Turbulence on the Flow Around Bluff Bodies," *Euromech 160: Periodic Flow and Wake Phenomena*, Berlin, 1982.
- ³Kiya, M., and Sasaki, K., "Freestream Turbulence Effects on a Separation Bubble," *Journal of Wind Engineering and Industrial Aerodynamics*, Vol. 14, 1983, pp. 375-386.
- ⁴Dziomba, B., "Experimental Investigation of Bluff Body Separation Regions," CASI Aerodynamics Symposium, Montréal, Canada, 1985.
- ⁵Ota, T., Asano, Y., and Okawa, J., "Reattachment Length and Transition of the Separated Flow Over Blunt Flat Plates," *Bulletin of the Japan Society of Mechanical Engineers*, Vol. 24, June 1981, pp. 941-947.
- ⁶Djilali, N., and Gartshore, I. S., "Turbulent Flow Around a Bluff Rectangular Plate. Pt. 1: Experimental Investigations," *ASME Journal of Fluids Engineering*, Vol. 113, No. 1, 1991, pp. 51-59.
- ⁷Castro, I. P., and Dianat, M., "The Pulsed-Wire Skin-Friction Measurement Technique," *Proceedings of the 5th Symposium on Turbulent Shear Flows*, Cornell Univ., Ithaca, NY, 1985, pp. 11.19-11.24.
- ⁸Roshko, A., and Lau, J. C., "Some Observations on Transition and Reattachment of a Free Shear Layer in Incompressible Flow," *Proceedings of the Heat Transfer and Fluid Mechanics Institute*,

edited by A. F. Charwatt, Stanford Univ. Press, Stanford, CA, 1965, pp. 157-167.

⁹Ruderich, R., and Fernholz, H. H., "An Experimental Investigation of a Turbulent Shear Flow with Separation, Reverse Flow, and Reattachment," *Journal of Fluid Mechanics*, Vol. 163, Feb. 1986, pp. 283-322.

¹⁰Westphal, R. V., Johnston, J. P., and Eaton, J. K., "Experimental Study of Flow Reattachment in a Single-Sided Sudden Expansion," NASA CR-3765, 1984.

¹¹Simpson, R. L., "Two-Dimensional Turbulent Separated Flow," AGARDograph 287, 1985.

Prandtl-Meyer Function for Dense Gases

M. S. Cramer* and A. B. Crickenberger†

Virginia Polytechnic Institute and State University,
Blacksburg, Virginia 24061

I. Introduction

THE Prandtl-Meyer function plays a central role in the analysis of many steady isentropic flows. The restriction to perfect gases, i.e., those satisfying

$$p = \rho RT \quad \text{with} \quad c_v = \text{const} \quad (1)$$

where p , ρ , R , T , and c_v are the thermodynamic pressure, fluid density, gas constant, absolute temperature, and the specific heat at constant volume, respectively, permits the derivation of explicit formulas for the Prandtl-Meyer function. However, many applications require consideration of dense gas effects. Examples include many industrial and chemical processing systems, power systems, typically those based on the Rankine cycle, and some wind-tunnel designs. The latter take advantage of the large decrease in kinematic viscosity, due both to choice of working fluid and operation at higher pressure, to increase the Reynolds number for a given Mach number.

An important dense gas effect exhibited by many fluids is a decrease in the sound speed during isentropic compression. A nondimensional parameter measuring the variation of sound speed along an isentrope is

$$\tilde{\Gamma} \equiv 1 + \frac{\rho}{a} \frac{\partial a}{\partial \rho} \bigg|_s \quad (2)$$

where

$$a \equiv \left(\frac{\partial p}{\partial \rho} \bigg|_s \right)^{1/2} \quad (3)$$

is the thermodynamic sound speed and s is the fluid entropy. The thermodynamic quantity $\tilde{\Gamma}$ has been termed the fundamental derivative of gasdynamics by Thompson,¹ who demonstrated its significance in virtually all areas of gasdynamics. It is easily verified that

$$\tilde{\Gamma} = \frac{\gamma + 1}{2} > 1 \quad (4)$$

Received Aug. 22, 1990; revision received April 5, 1991; accepted for publication April 12 1991. Copyright © 1991 by the American Institute of Aeronautics and Astronautics, Inc. All rights reserved.

*Associate Professor, Department of Engineering Science and Mechanics. Member AIAA.

†Graduate Project Assistant, Department of Engineering Science and Mechanics.

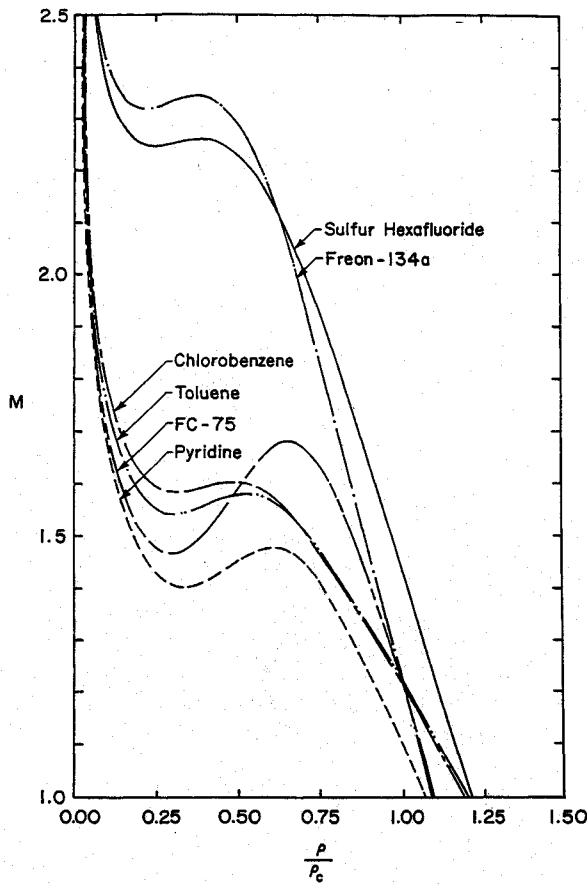


Fig. 1 Computed Mach number variation along isentropes (stagnation properties are given in Table 1).

if the gas is perfect, from which we recover the well-known conclusion of the perfect gas theory that the sound speed increases with density and pressure along an isentrope. Here, γ is the ratio of specific heats. However, most fluids, including water vapor, have $\bar{\Gamma} < 1$ in the dense gas regime, thus resulting in a decrease in sound speed during isentropic compression. For example, normal octane (C_8H_{18}) has a minimum value of $\bar{\Gamma}$ approximately equal to 0.4 on its critical isotherm.

Cramer² and Cramer and Best³ have demonstrated that the Mach number may have local extrema in the course of an isentropic expansion. This, of course, is in marked contrast with the behavior of perfect gases in which the Mach number decreases monotonically with increasing density or pressure in an isentropic flow. These local extrema and the region of increasing Mach number are illustrated in Fig. 1; the details of these computations are described in the following sections. The purpose of the present study is to demonstrate that these mechanisms also result in nonclassical behavior of the Prandtl-Meyer function. In particular, we show that the Prandtl-Meyer functions of fluids that have $\bar{\Gamma} < 1$ in some region of their thermodynamic space may be multivalued functions of the Mach number M . We recall that this contrasts with the behavior of perfect gases in which the Prandtl-Meyer function increases monotonically with Mach number.

II. Formulation

We restrict our attention to flows that are classical in the sense that they are single phase and in equilibrium. In the usual way, these flows are taken to be isentropic and steady. As a result the fluid motion is governed by the Bernoulli equation

$$h + \frac{a^2 M^2}{2} = \text{const} \quad (5)$$

Table 1 Stagnation states corresponding to isentropes of Figs. 1 and 2 (subscripts o and c denote stagnation and critical states, respectively)

Fluid	V_o/V_c	T_o/T_c	p_o/p_c
Sulfur hexafluoride	0.67	1.20	4.97
Freon-134a	0.67	1.23	5.73
Toluene	0.67	1.07	2.01
Pyridine	0.70	1.05	1.66
Chlorobenzene	0.67	1.08	2.13
FC-75	0.70	1.05	2.00

and the condition of isentropic flow

$$s = \text{const} \quad (6)$$

Here, $h = h(\rho, s)$ is the fluid enthalpy and M is the Mach number. A definition of the Prandtl-Meyer function that is valid at all densities is

$$\nu \equiv \nu_r - \int_{\rho_r}^{\rho} \frac{(M^2 - 1)^{1/2}}{M^2} \frac{d\rho}{\rho} \quad (7)$$

where the subscript r refers to some reference state. The integrand in Eq. (7) can be cast as a pure function of density through use of Eqs. (5) and (6) supplemented with the equation of state. A result similar to Eq. (7) may be found in most standard references on gasdynamics, see, e.g., Thompson⁴ or Anderson.⁵ If Eqs. (5-7) are combined with the perfect gas model (1), the well-known results for $\nu(M, \gamma)$ are obtained. In the dense gas regime, Eq. (1) no longer gives an accurate representation of the fluid behavior and more complex equations of state will be necessary. In such cases, Eq. (7) must be integrated numerically. For this reason, Eqs. (5-7) will be cast as the following system of ordinary differential equations:

$$\frac{d\nu}{dV} = \frac{(M^2 - 1)^{1/2}}{VM^2} \quad (8)$$

$$\frac{dM}{dV} = -\frac{M}{V} J \quad (9)$$

$$\frac{dT}{dV} = -\frac{T p_T}{c_v} \quad (10)$$

where $V \equiv \rho^{-1}$ is the specific volume,

$$p_T \equiv \frac{\partial p}{\partial T}(V, T) \quad (11)$$

$$J \equiv 1 - \bar{\Gamma} - M^{-2} \quad (12)$$

Equation (8) is recognized as the differential form of the basic definition (7). Equation (9) was derived by combining the definitions (2) and (3) with the thermodynamic identity

$$\left. \frac{\partial h}{\partial \rho} \right|_s = \frac{a}{\rho}$$

and the differential of Eqs. (5) and (6). A result similar to Eq. (9) has also been employed by Thompson,¹ Cramer,² and Cramer and Best.³ Equation (10) ensures that the isentropic condition is satisfied. The differential system (8-12) is solvable once the thermodynamic functions

$$\bar{\Gamma} = \bar{\Gamma}(V, T), \quad p_T = p_T(V, T), \quad c_v = c_v(V, T) \quad (13)$$

are determined by the gas model. The initial conditions will be taken to be

$$\nu = 0, \quad M = 1, \quad T = T_* \quad \text{at} \quad V = V_* \quad (14)$$

where the asterisks refer to sonic conditions. The integrations were carried out through use of a standard sixth-order Runge-Kutta scheme.

In practice, we found it convenient to first choose a stagnation state (T_o, V_o). Equations (9-12) were then employed to ascertain T^* and V^* . Thus, in Sec. IV, each case is identified by its stagnation state.

As discussed by Cramer² and Cramer and Best,³ the nonclassical behavior is expected when $J > 0$. When this is the case, the Mach number decreases with V and therefore increases with ρ or p . Inspection of Eqs. (7) or (8) reveals that ν decreases with ρ . Thus, ν will decrease with M if $J > 0$. We further note that the condition $J > 0$ is only possible if $\bar{\Gamma} < 1$ over a range of pressures and temperatures. From Eq. (4), it is clear that this condition cannot be satisfied by perfect gases. In fact, it may be shown that

$$J = -\frac{1 + [(\gamma - 1)/2]M^2}{M^2} < 0$$

if the gas is perfect. A simple numerical example of the nonclassical behavior is an isentropic flow that attains the condition $\bar{\Gamma} = 0.6$ at some point in the flow. If the Mach number is specified to be $> (2.5)^{1/2} \approx 1.58$, then $J > 0$ there and $J < 0$ if $1 < M < 1.58$ there. More general arguments have been provided by Cramer² and Cramer and Best,³ who showed that a $J > 0$ region can always be attained if the fluid admits a region of $\bar{\Gamma} < 1$ and the stagnation pressure is taken to be sufficiently large.

III. Fluids and Gas Models

The fluids chosen to illustrate the nonclassical behavior of ν are sulfur hexafluoride (SF_6), Freon-134a ($\text{C}_2\text{H}_2\text{F}_4$), toluene (C_7H_8), pyridine ($\text{C}_5\text{H}_5\text{N}$), chlorobenzene ($\text{C}_6\text{H}_5\text{Cl}$), and perfluoro-2-butyltetrahydrofuran ($\text{C}_8\text{F}_{16}\text{O}$). The latter will be referred to by its trade name FC-75. The last four fluids are already in widespread use as working fluids for organic Rankine cycles, see, e.g. the report by Miller⁶ or the more

Table 2 Computed Prandtl-Meyer function, Mach number, and density variation for simple expansive flow along the isentropes of Figs. 1 and 2 (fluid is pyridine)

θ , deg	ν	M	ρ/ρ_c
0	0.364	1.45	0.492
-5	0.452	1.42	0.414
-10	0.539	1.40	0.347
-15	0.626	1.41	0.245
-20	0.713	1.43	0.291
-25	0.801	1.47	0.206

recent reviews by Curran⁷ and Manco and Nervegna.⁸ Sulfur hexafluoride was chosen for its potential in wind-tunnel applications, see, e.g., Anderson.⁹ Freon-134a belongs to the new class of chlorine-free Freons and is also under consideration for wind-tunnel work.¹⁰ One advantage of the fluids considered here is that their properties are well documented. The critical properties, boiling temperature, and ideal gas specific heat for sulfur hexafluoride, toluene, pyridine, and chlorobenzene were all obtained from Reid et al.¹¹ Data for Freon-134a were obtained directly from the manufacturer's (DuPont Co.) literature, and data for FC-75 were taken from Yarrington and Kay.¹²

A complete gas model is obtained by specifying the equation of state, typically of the form $p = p(V, T)$, and the temperature dependence of the ideal gas specific heat defined by

$$c_{v\infty} = c_{v\infty}(T) \equiv \lim_{V \rightarrow \infty} c_v(V, T) \quad (15)$$

The equation of state employed for all but one of the fluids described here is the highly accurate model developed by Martin and Hou.¹³ Because of its analytical basis, the Martin-Hou equation requires only a minimum number of physical parameters characterizing the specific substance. These are the critical pressure, temperature, and specific volume and the boiling temperature. Comparisons with the extensive thermodynamic data of Yarrington and Kay¹² indicate that the results for FC-75 are in error by no more than 3%, with 1-2% being typical in the temperature and pressure ranges of interest here. Similar results were found for water, and we expect the errors for the remaining fluids are of the same order of magnitude. The literature for Freon-134a distributed by the manufacturer employs the well-known Redlich-Kwong equation of state; we have also employed this equation for this fluid. A discussion of the Redlich-Kwong equation may be found in any standard reference on thermodynamics, see, e.g., Van Wylen and Sonntag.¹⁴ The main difference between our pressure estimates and those of the manufacturer appear to be due to slight differences in the input parameters; these differences appear to be no more than 1% over all temperatures and pressures considered.

To simplify the computations, the ideal gas specific heat [Eq. (15)] was approximated as a power law, i.e., $c_{v\infty} \propto T^n$. This simplification yields very accurate results over the limited temperature range used here. For example, we consider chlorobenzene and note that the difference between the power law estimate and that given by the cubic of Reid et al.¹¹ is no more than 2% over a range of 500-700 K.

The quantities $c_v(V, T)$ and $\bar{\Gamma}(V, T)$ required in Eqs. (8-10) may be derived by standard thermodynamic manipulations. Explicit expressions may be found in Thompson and Lambrakis¹⁵ or Cramer.¹⁶

In order to check that the flows considered remained in the single-phase regime, the saturated vapor line was estimated through use of Riedel's¹⁷ vapor pressure equation. Tests employing the known data for water, Freon-134a, and FC-75

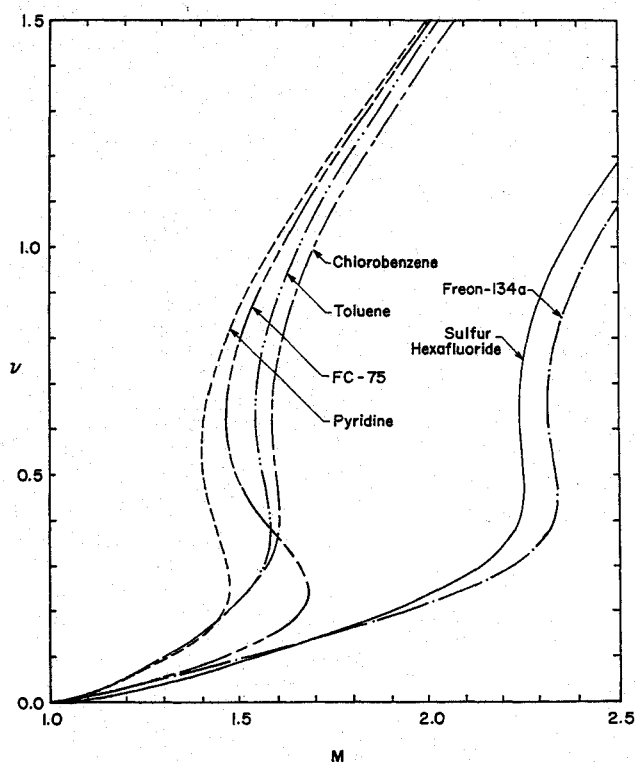


Fig. 2 Computed Prandtl-Meyer functions along the isentropes of Fig. 1 (the units for the Prandtl-Meyer functions are radians).

show that estimates based on Riedel's approximation differ from the accepted or published data by only 1–2% in the flow regimes of interest.

All results shown were found to be in the single-phase regime. It turns out that the main difficulties with respect to violation of the single-phase assumption were in the calculations involving Freon-134a and SF₆. Both fluids are similar to water in that they are wetting, i.e., isentropic expansion of vapors having $T < T_c$ results in condensation. A detailed examination of the numerical results shows that the intersection of the isentropes with the saturated vapor lines occurs at lower densities than those considered here. The remaining fluids, chlorobenzene, toluene, FC-75, and pyridine, are all retrograde or drying fluids, see, e.g., Curran⁷ or Manco and Nervegna,⁸ in that the thermodynamic state moves away from the saturation curve under isentropic expansion. In such fluids, condensation of a vapor typically requires isentropic compression rather than expansion. Thus, isentropes originally in the single-phase region tended to remain there in the calculations involving the latter fluids.

IV. Results

The results of the straightforward numerical integration of Eqs. (8–10) are displayed in Figs. 1 and 2. The stagnation properties of each isentrope are listed in Table 1. The region of increasing Mach number with ρ is clearly evident in Fig. 1. As discussed in Sec. II, the Prandtl-Meyer functions decrease with increasing M for this range of Mach numbers. In order to further illustrate the anti-intuitive nature of these results, we consider an expansive flow of pyridine. The stagnation properties of the flow will be identical to those of Figs. 1 and 2 and indicated in Table 1. The undisturbed flow will be taken to be horizontal and uniform at a density of $0.492\rho_c$ and a Mach number of 1.45. This state is just to the left of the local maximum in M in Fig. 1 and just above the local maximum in M in Fig. 2. Because this is a simple wave region, the Mach number can be related to the flow deflection angle by the usual characteristic relation

$$\nu(M) = \nu(M_\infty) - \theta$$

where M_∞ is the Mach number of the undisturbed flow and θ is measured counterclockwise from the undisturbed flow direction. From Fig. 2, it is clear that M is a single-valued function of ν . The Prandtl-Meyer function, Mach number, and density for a selection of flow deflection angles corresponding to expansive flows have been computed and are displayed in Table 2. Here we may think of the expansion as being caused by a sharp expansive corner; this, of course, results in a Prandtl-Meyer expansion fan. Then each case in Table 2 corresponds to a different corner angle. On the other hand, we may also regard this series as different stages of a gradual expansion. Although this is a textbook flow in its simplicity, the decrease in sound speed leads to a decrease, rather than the increase of the perfect gas theory, in Mach number during the expansion. It should be noted that this turning of the flow does in fact expand the flow, i.e., ρ , and, therefore, p decreases with decreasing θ as in the case of perfect gases. For the cases shown, the local minimum in M has been attained at $M \approx 1.4$. The Mach number then increases and exceeds the original Mach number for $|\theta| > 23$ deg.

V. Summary

The preceding has given a brief description of the nonclassical behavior of the Prandtl-Meyer function to be expected in the dense gas regime. The Prandtl-Meyer function is seen to decrease, rather than increase, with Mach number at densities, temperatures, and Mach numbers such that J , as defined in Eq. (12), is positive. The results of the present study indicate

the $J > 0$ condition is easily attainable for fluids commonly encountered in applications.

It is useful to note that these effects are expected to occur only at pressures and temperatures corresponding to the dense gas regime. At lower pressures and densities, the gas behavior is accurately predicted by Eq. (1) and the well-known results for ν are recovered. Furthermore, as the molecular weight and complexity of the fluid increases, the fundamental derivative decreases and the aforementioned effects appear to become more pronounced. Thus, one expects the nonclassical behavior to be characteristic of heavier hydrocarbons and fluorocarbons rather than lighter substances such as helium or molecular nitrogen.

The importance of the effect described here is obvious when considering computations involving the method of characteristics. However, the example provided in the last section demonstrates that the nonclassical behavior must also be considered in other computational or experimental studies. Without a recognition of this effect, a computed or measured decrease in the Mach number in an expansive flow or, for that matter, an increase in the Mach number in an isentropic compression may be misinterpreted as due to error in the experimental method, numerical scheme, or the equation of state. The work presented here shows that these nonclassical effects are due to the natural dynamics of fluids having a nonmonotone sound speed variation.

Acknowledgment

This work was supported by the National Science Foundation under Grant CTS-8913198.

References

- Thompson, P. A., "A Fundamental Derivative in Fluids," *Physics of Fluids*, Vol. 14, No. 9, 1971, pp. 1843–1849.
- Cramer, M. S., "Nonclassical Dynamics of Classical Gases," *Nonlinear Waves in Real Fluids*, edited by A. Kluwick, Springer-Verlag, New York, 1991.
- Cramer, M. S., and Best, L. M., "Steady, Isentropic Flows of Dense Gases," *Physics of Fluids A*, Vol. 3, No. 1, 1991, pp. 219–226.
- Thompson, P. A., *Compressible-Fluid Dynamics*, McGraw-Hill, 1972.
- Anderson, J. D., *Modern Compressible Flow with Historical Perspective*, McGraw-Hill, New York, 1982.
- Miller, D. R., "Rankine Cycle Working Fluids for Solar-to-Electrical Energy Conversion," Sandia Laboratories, Albuquerque, NM, Energy Report SLA-74-0132, 1974.
- Curran, H. M., "Use of Organic Working Fluids in Rankine Engines," *Journal of Energy*, Vol. 5, No. 4, 1981, pp. 218–223.
- Manco, S., and Nervegna, N., "Working Fluid Selection via Computer Assisted Analysis of ORC Waste Heat Recovery Systems," Society of Automotive Engineers, Paper P-85-164, 1985.
- Anderson, W. K., "A Numerical Study on the Use of Sulfur Hexafluoride (SF₆) as a Test Gas for Wind Tunnels," AIAA 16th Aerodynamics Ground Testing Conference, Seattle, WA, June 1990.
- Anderson, W. K., private communication, 1990.
- Reid, R. C., Prausnitz, J. M., and Poling, B. E., *The Properties of Gases & Liquids*, 4th ed., McGraw-Hill, New York, 1987.
- Yarrington, R. M., and Kay, W. B., "Thermodynamic Properties of Perfluoro-2-Butyltetrahydrofuran," *Journal of Chemical Engineering Data*, Vol. 5, No. 1, 1960, pp. 24–29.
- Martin, J. J., and Hou, Y. C., "Development of an Equation of State for Gases," *AIChE Journal*, Vol. 1, No. 2, 1955, pp. 142–151.
- Van Wylen, G. J., and Sonntag, R. E., *Fundamentals of Classical Thermodynamics*, 3rd ed., Wiley, New York, 1985.
- Thompson, P. A., and Lambrakis, K. C., "Negative Shock Waves," *Journal of Fluid Mechanics*, Vol. 60, 1973 pp. 187–208.
- Cramer, M. S., "Negative Nonlinearity in Selected Fluorocarbons," *Physics of Fluids A*, Vol. 1, No. 11, 1989, pp. 1894–1897.
- Riedel, L., "Eine neue Universelle Dampfdruckformel-Untersuchungen über eine Erweiterung des Theorems der übereinstimmenden Zustände. Teil 1," *Chemische Ingenieure Technik*, Vol. 26, 1954, p. 83.